

GAMMA-GAMMA, GAMMA-ELECTRON COLLIDERS *

Valery Telnov

Institute of Nuclear Physics, Novosibirsk, Russia[†]
and KEK, Japan

Abstract

It is very likely that in 3-4 years the construction of one or two linear colliders with c.m.s energy up to 0.5–1.5 TeV will be started. Besides e^+e^- collisions, linear colliders give a unique possibility to study $\gamma\gamma$ and γe interactions at energies and luminosities comparable to those in e^+e^- collisions. High energy photons for $\gamma\gamma$ and γe collisions can be obtained using laser backscattering. These types of collisions considerably increase the physics potential of linear colliders for relatively a small incremental cost. This report briefly reviews the physics goals of $\gamma\gamma$, γe colliders and possible parameters of photon-photon colliders.

1 INTRODUCTION

The possibility of obtaining $\gamma\gamma$, γe colliding beams with high energy and luminosity using Compton scattering of laser light on high energy electrons at linear colliders (LC) has been considered since 1981 [1–5]. Possible parameters and physics potential of such colliders has been discussed at many Workshops on LC and at the Workshop on Gamma-Gamma colliders held in Berkeley in 1994 [6]. Physics phenomena which can be studied in $\gamma\gamma$, γe collisions with high energies has been considered in many hundreds of papers. This option is included now in the Conceptual Design Reports of the NLC [7], TESLA–SBLC [8], and JLC [9] linear colliders. All these projects foresee a second interaction region for $\gamma\gamma$, γe collisions.

However, in our time of tight HEP budgets the physics community needs a very clear understanding whether $\gamma\gamma$, γe collisions can really give new physics information in addition to e^+e^- collisions that could justify an additional collider cost ($\sim 20\%$, including detector). In general, the physics at e^+e^- and $\gamma\gamma$, γe colliders is quite similar but complimentary, because cross sections depend differently on new unknown physics parameters. Roughly, the answer to the previous question depends on the number of produced

interesting events (cross section \times luminosity). If the statistics are comparable, then $\gamma\gamma$, γe colliders should be built together with e^+e^- colliders without a doubt. In my opinion, this condition is satisfied. Moreover, the beam collision effects allow more than one order further increase of $\gamma\gamma$ luminosity though this will need upgrading of the injector (decrease of the product of transverse beam emittances).

The basic scheme of a photon collider is shown in Figs. 1 and 2. Two electron beams after the final fo-

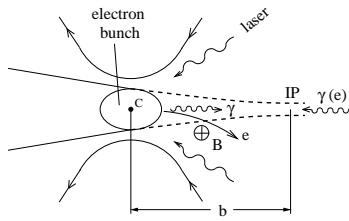


Figure 1: Scheme of $\gamma\gamma$, γe collider.

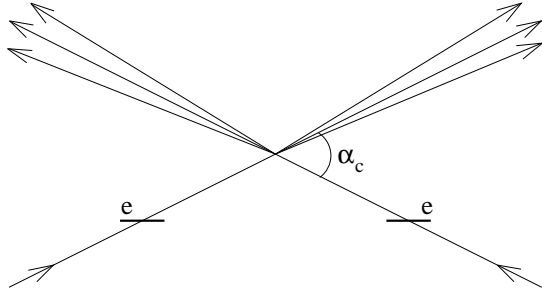


Figure 2: Crab-crossing scheme

cus system are traveling toward the interaction point (IP) and at a distance of about 0.1–1 cm from the IP collide with the focused laser beams. Photons after Compton scattering have energies comparable with the energies of the initial electrons and follow their direction (to the IP) with some small additional angular spread of the order $1/\gamma$. With reasonable laser parameters one can “convert” most of the electrons into high energy photons. The luminosity of $\gamma\gamma$, γe collisions will be of the same order of magnitude as the “geometric” luminosity of the basic ee beams. Luminosity distributions in $\gamma\gamma$ collisions have characteristic peaks near the maximum invariant masses

*Invited talk at XII Intern. conf. on High Energy Accelerators (HEACC'98), Sept.7-12, 1998, Dubna, Russia

[†]permanent address, email:telnov@inp.nsk.su

with a typical width about 10 % (and a few times smaller in γe collisions). High energy photons can have various polarizations, which is very advantageous for experiments.

In the conversion region a photon with an energy ω_0 is scattered on an electron with an energy E_0 at a small collision angle α_0 (almost head-on). The energy of the scattered photon ω depends on its angle ϑ with respect to the motion of the incident electron as follows:

$$\omega = \frac{\omega_m}{1 + (\vartheta/\vartheta_0)^2}; \quad \omega_m = \frac{x}{x+1} E_0; \quad \vartheta_0 = \frac{mc^2}{E_0} \sqrt{x+1},$$

$$x = \frac{4E_0\omega_0 \cos^2 \alpha_0/2}{m^2 c^4} \simeq 15.3 \left[\frac{E_0}{TeV} \right] \left[\frac{\omega_0}{eV} \right], \quad (1)$$

where ω_m is the maximum photon energy,

For example: $E_0 = 300$ GeV, $\omega_0 = 1.17$ eV (neodymium glass laser) $\Rightarrow x = 5.37$ and $\omega/E_0 = 0.84$. The value $x = 4.8$ is the threshold for e^+e^- production in collision of the high energy electron with a laser photon. Above this threshold ($x = 6-15$) the yield of high energy photons will be lower by a factor 2–2.5. Corresponding formulae and graphs can be found elsewhere [2–5].

2 PHYSICS

The physics at high energy $\gamma\gamma$, γe colliders is very rich and no less interesting than that in e^+e^- or pp collisions:

1. The Higgs boson (which is thought to be responsible for the origin of particle masses) will be produced at photon colliders as a single resonance. The cross section is proportional to the two-photon decay width of the Higgs boson which is sensitive to all heavy charged particles (even super-heavy) which get their mass via the Higgs mechanism. In addition, some Higgs decay modes and its mass can be measured at $\gamma\gamma$ colliders more precisely than in e^+e^- collisions due to larger production cross sections and the very sharp edge of the luminosity spectrum.

2. Cross sections for production of charged scalar, lepton and top pairs in $\gamma\gamma$ collisions are larger than those in e^+e^- collisions by a factor of approximately 5–10; for WW production this factor is even larger, about 10–20.

3. In γe collisions, charged supersymmetric particles with masses higher than in e^+e^- collisions can be produced (a heavy charged particle plus a light neutral); $\gamma\gamma$ collisions also provide higher accessible masses for particles which are produced as a single resonance in $\gamma\gamma$ collisions (such as the Higgs boson).

The most interesting (expected) physics at next linear colliders is the search for and study of the Higgs boson(s) and supersymmetric particles. Photon colliders can make a considerable contribution to this physics.

The mass of the Higgs most probably lies in the region of $100 < M_H < 300$ GeV. The effective cross section is presented in fig. 3 [10]. Note that here $L_{\gamma\gamma}$

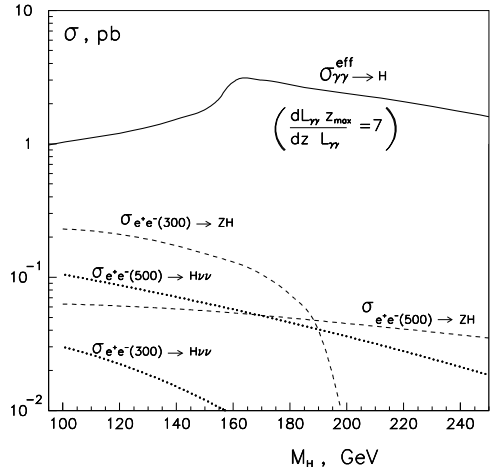


Figure 3: Cross sections for the Standard model Higgs in $\gamma\gamma$ and e^+e^- collisions.

is defined as the $\gamma\gamma$ luminosity at the high energy luminosity peak ($z = W_{\gamma\gamma}/2E_e > 0.65$ for $x = 4.8$) with FWHM about 15%. The luminosity in this peak is approximately equal to $0.25k^2 L_{ee}(\text{geom})$ (k is the conversion coefficient). For comparison, in the same figure the cross sections of the Higgs production in e^+e^- collisions are shown.

We see that for $M_H = 120-250$ GeV the effective cross section in $\gamma\gamma$ collisions is larger than that in e^+e^- collisions by a factor of about 6–30! If the Higgs is light enough, its width is much less than the energy spread in $\gamma\gamma$ collisions. It can be detected as a peak in the invariant mass distribution or can be searched by energy scanning using the very sharp edge of luminosity distribution (see fig.4). Observation of a sharp step in the visible cross section will imply narrow resonance production with subsequent decay in the considered channel. This method is very attractive for study of the Higgs in the $\tau\tau$ decay mode where direct reconstruction is impossible due to undetected neutrinos while it can be seen as a step in visible cross section for events consisting of two low multiplicity collinear jets. The total number of events in the main decay channels $H \rightarrow b\bar{b}, WW(W^*), ZZ(Z^*)$ will be several thousands for a typical integrated luminosity of 10 fb^{-1} [10]. The scanning method also allows the

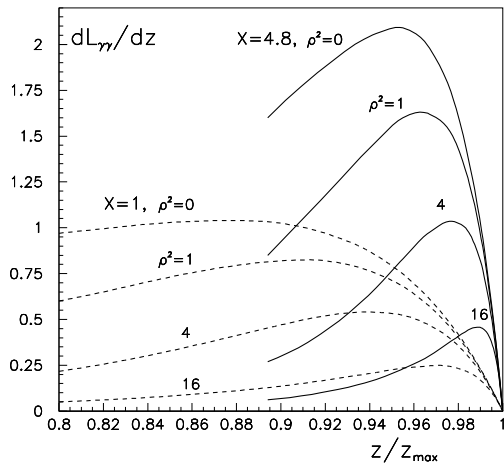


Figure 4: Shape of the $\gamma\gamma$ luminosity spectrum near the high energy edge.

measurement of the Higgs mass with high precision.

The second example is a charged pair production. The corresponding cross sections in unpolarized $\gamma\gamma$ and e^+e^- collisions are shown in Fig.5. One can see that in $\gamma\gamma$ collisions the cross sections are much larger, by at least a factor 5 for scalars and fermions and by about one order in WW channel. The cross section of scalar pair production (sleptons, for example) in collision of polarized photons is shown in fig.6. One can see that for heavy scalars the cross section in collisions of polarized photons is higher than that in e^+e^- collisions by a factor of 10–20.

3 LUMINOSITY OF $\gamma\gamma$ COLLIDERS IN CURRENT DESIGNS

3.1 0.5–1 TeV colliders

Below some results of simulation of $\gamma\gamma$ collisions at TESLA, ILC (converged NLC and JLC) and CLIC are presented. Beam parameters were taken the same as in e^+e^- collisions with the exception of horizontal beta function at IP, which is taken conservatively equal to 2 mm for all cases. In $\gamma\gamma$ collisions the beamstrahlung is absent and the horizontal size can be made much smaller than that in e^+e^- collisions. Minimum β_x is determined by the Oide effect (radiation in quads) which is included in the simulation code and also by technical problems connected with the chromatic corrections in both transverse directions – the limit here is not so clear. The conversion point(CP) is situated at the distance $b = \gamma\sigma_y$. It is assumed that electron beams have 85% longitudinal polarization and laser photons have 100% circular polarization.

The simulation code [5] takes into account all im-

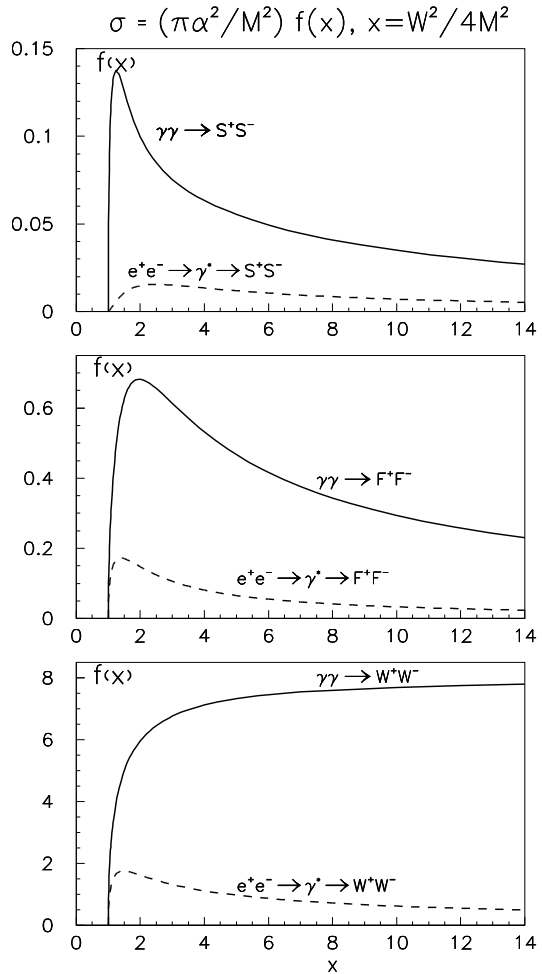


Figure 5: Cross sections for charged pair production in e^+e^- and $\gamma\gamma$ collisions. S (scalars), F (fermions), W (W-bosons); M is particle mass, W is invariant mass (c.m.s. energy of colliding beams)

portant processes: linear Compton scattering with all polarization effects, beamstrahlung (without polarization effects), coherent pair creation and interaction between charged particles.

We see that $\gamma\gamma$ luminosity in the hard part of the spectrum is $L_{\gamma\gamma}(z > 0.65) \sim 0.1L(\text{geom}) \sim (1/6)L_{e^+e^-}$.

Beside $\gamma\gamma$ collisions, there is considerable γe luminosity which adds some background (e^+e^- pairs in vertex detectors), but on the other hand, it is possible to study γe interactions simultaneously with $\gamma\gamma$ collisions. Optimization of $\gamma\gamma$ and γe luminosities was considered in refs.[4],[5],[8].

The normalized $\gamma\gamma$ luminosity spectra for a 0.5 TeV TESLA and ILC colliders are shown in Fig.7. The luminosity spectrum is decomposed into two parts, with total helicity of two photons 0 and 2.

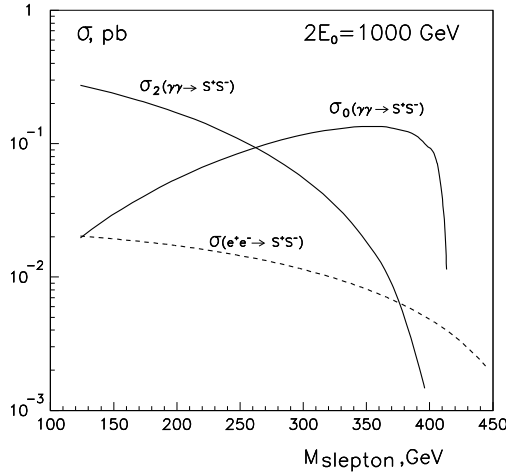


Figure 6: Cross sections for charged boson production in e^+e^- and $\gamma\gamma$ collisions at $2E_0 = 1$ TeV collider (in $\gamma\gamma$ collision $W_{max} \approx 0.82$ GeV ($x = 4.6$)); σ_0 and σ_2 correspond to the total $\gamma\gamma$ helicity 0 and 2.

Table 1: Parameters of $\gamma\gamma$ colliders based on Tesla(T), ILC(I) and CLIC(C).

	T(500)	I(500)	C(500)	T(800)	I(1000)	C(1000)
no deflection, $b = \gamma\sigma_y$, $x = 4.6$						
$N/10^{10}$	2.	0.95	0.4	1.4	0.95	0.4
σ_z , mm	0.4	0.12	0.05	0.3	0.12	0.05
$f_{rep} \times n_b$, kHz	15	11.4	30.1	13.5	11.4	26.6
$\gamma\epsilon_{x,y}/10^{-6}$, m-rad	10/0.03	5/0.1	1.9/0.1	8/0.01	5/0.1	1.5/0.1
$\beta_{x,y}$, mm at IP	2/0.4	2/0.12	2/0.1	2/0.3	2/0.16	2/0.1
$\sigma_{x,y}$, nm	200/5	140/5	88/4.5	140/2	100/4	55/3.2
b , mm	2.4	2.4	2.2	1.5	4	3.1
$L(geom)$, 10^{33}	48	12	10	75	20	19.5
$L_{\gamma\gamma}(z > 0.65)$, 10^{33}	4.5	1.1	1.05	7.2	1.75	1.8
$L_{\gamma e}(z > 0.65)$, 10^{33}	6.6	2.6	2.8	8	4.2	4.6
L_{ee} , 10^{33}	1.2	1.2	1.6	1.1	1.8	2.3
$\theta_x/\theta_{y,max}$, mrad	5.8/6.5	6.5/6.9	6/7	4.6/5	4.6/5.3	4.6/5.5

We see that in the high energy part of the luminosity spectra photons have high degree of polarization, which is very important for many experiments. In addition to the high energy peak, there is a factor 5–8 larger low energy luminosity. It is produced by photons after multiple Compton scatterings and beamstrahlung photons. Fortunately, these event have large boost and can be easily distinguished from the central high energy events.

Fig.8 (upper) shows the same spectrum with an additional cut on the longitudinal momentum of the produced system which suppresses low energy luminosity to a negligible level. Fig.8 (lower) shows the same spectrum with a stronger cut on the longitudinal momentum. In this case the spectrum has a nice peak with FWHM about 7.5%. Of course, such

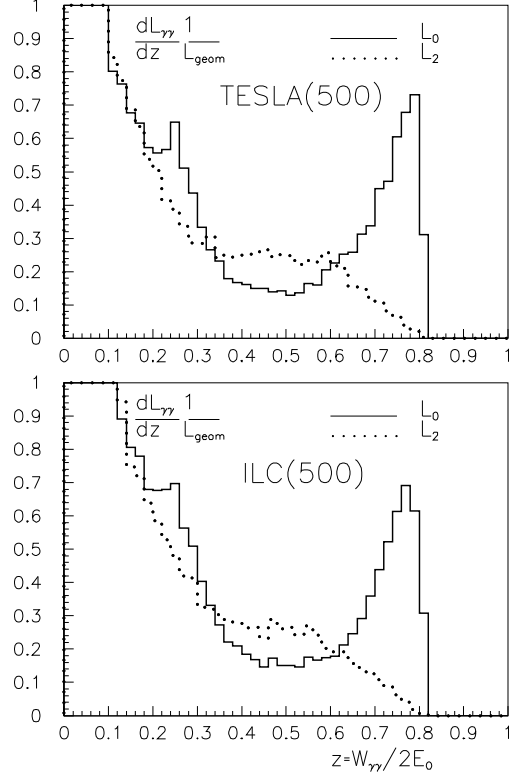


Figure 7: Luminosity spectra for $\gamma\gamma$ collisions for collider parameters presented in table 1. Solid line for total helicity of two photons 0 and dotted line for total helicity 2.

procedure is somewhat artificial because instead of such cuts one can directly selects events with high invariant masses, the minimum width of the invariant mass distribution depends only on the detector resolution. However, there are very important examples when one can obtain a “collider resolution” somewhat better than the detector resolution, such as the case of only two jets in the event when one can restrict the longitudinal momentum of the produced system using the acollinearity angle between jets ($H \rightarrow b\bar{b}, \tau\bar{\tau}$, for example).

Detailed background studies [8] show that the low energy part ($z < 0.6$) of the $\gamma\gamma$ luminosity increases hadronic background in the detector by only a factor of 2. In the scheme with deflection of electrons by the magnetic field of a small magnet between IP and CP it is possible to suppress the low energy part of the $\gamma\gamma$ luminosity by several times — however, this approach is more complicated technically and the maximum $\gamma\gamma$ luminosity is smaller than that without deflection (due to the larger space between CP and IP).

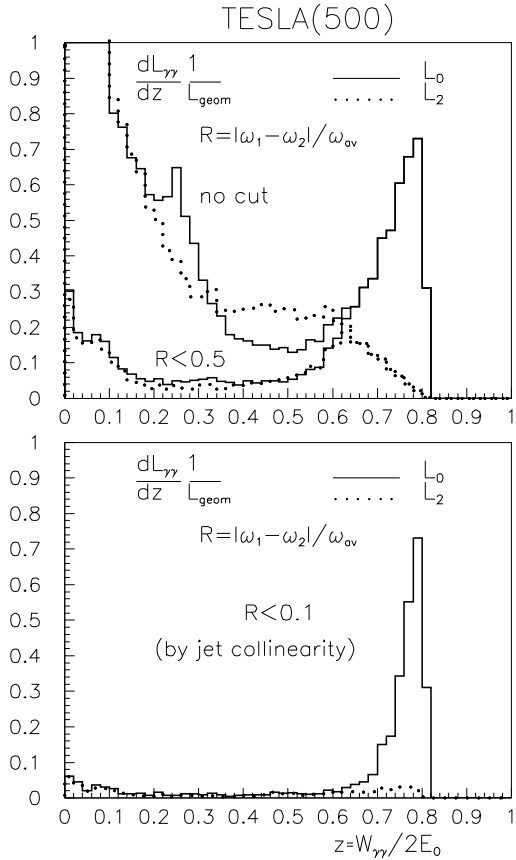


Figure 8: Luminosity spectra for $\gamma\gamma$ collisions at TESLA(500) with various cut on the relative difference of the photon energy. See comments in the text.

3.2 $\gamma\gamma$ collider for low mass Higgs

It is very possible that the Higgs boson has a mass in the region 115-150 GeV as predicted in some theories. It is of interest to consider possible parameters of a $\gamma\gamma$ collider based on TESLA and ILC at these energies. Two variants were considered for $H(130)$: 1) the ‘‘Compton’’ parameter x is fixed near the threshold of e^+e^- creation ($x \approx 4.6$), which corresponds to $\lambda \sim 325$ nm and $E_0 = 79$ GeV; 2) the laser is the same as for $2E_0 = 500$ GeV colliders, namely a Nd:glass laser with $\lambda = 1.06 \mu\text{m}$, which corresponds to $x = 1.8$ and $E_0 = 100$ GeV. All other beam parameters are taken the same as for $2E_0 = 500$ GeV (see Table 1). Results of simulation for these two cases are shown in Table 2 (TESLA and ILC) and in Fig.9 (TESLA). Comparing these two variants we see that peak luminosities (dL/dz) are approximately the same (note that L_{geom} at $x = 1.8$ is larger by a factor 1.26 due to larger energy), and the ratio L_0/L_2 is also the same (the Higgs is produced by L_0 and main backgrounds comes from L_2). The only difference is that the slope of the luminosity at

Table 2: Parameters of the $\gamma\gamma$ colliders for $H(130)$ at TESLA(T) and ILC(I).

	T(2x79)	I(2x79)	T(2x100)	I(2x100)
$x = 1.8$			$x = 4.6$	
$\sigma_{x,y, \text{nm}}$	320/7.8	230/7.8	360/8.8	250/8.8
b, mm	1.5	1.5	1.4	1.4
$L(\text{geom}), 10^{33}$	19	4.6	15	3.7
$L_{\gamma\gamma}(z/z_m > 0.8), 10^{33}$	1.55	0.37	1.45	0.35
$L_{e^+e^-}(z/z_m > 0.8), 10^{33}$	3.	1.45	1.7	1.3
$\theta_x/\theta_y, \text{mrad}$	5.2/6.2	5.2/7	$\sim 10/12$	$\sim 10/12$

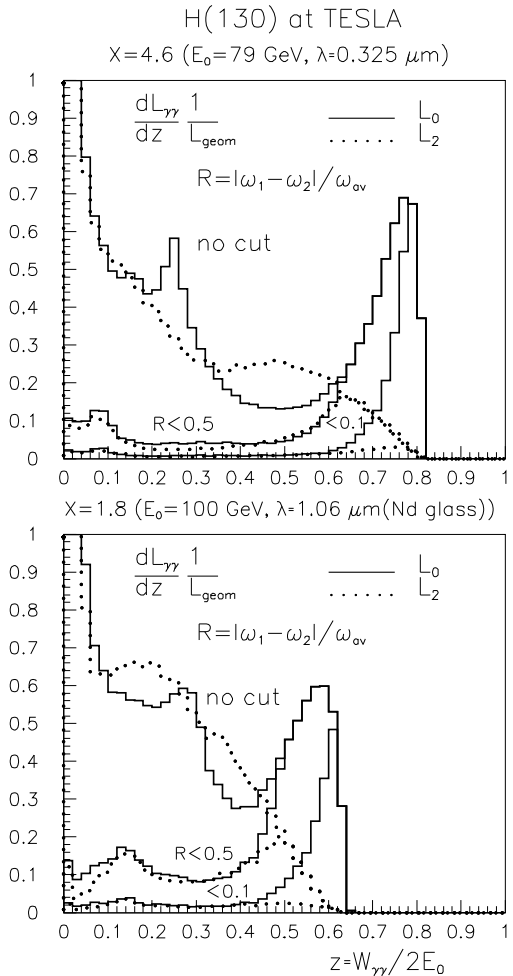


Figure 9: Luminosity spectra of $\gamma\gamma$ collision of ‘low’ energy $\gamma\gamma$ collider (TESLA beam parameters) for study of the Higgs with a mass $M_H = 130$ GeV, upper figure for $x = 4.8$ and lower for $x = 1.8$ (the same laser as for $2E_0 = 500$ GeV).

z near z_{max} is larger for $x = 4.6$ by a factor 2.3 (important for measurement of Higgs mass). Also the maximum disruption angle at $x = 4.8$ is larger by a factor 1.7. This angle determines the minimum crab crossing angle at the interaction point (see Fig.2).

For $2E=500$ GeV colliders the maximum disruption angle is 10 mrad (safely) and the crab-crossing angle $\alpha_c = 30$ mrad. If we keep $x = const$, then at $2E_0 = 2 \times 79$ GeV the maximum disruption angle will be larger by a factor $\sqrt{250/79} = 1.8$, which already introduces some problems.

From this consideration we can conclude that one can use the same Nd:glass laser at all energies below $2E_0 \sim 500$ GeV.

4 ULTIMATE $\gamma\gamma$ LUMINOSITY

The $\gamma\gamma$ luminosities in the current projects are determined by the “geometric” luminosity of the electron beams. The only collision effect restricting the maximum value of the $\gamma\gamma$ luminosity is coherent pair creation when the high energy photon is converted into an e^+e^- pair in the field of the opposing electron beam [11],[4],[5]. Having electron beams with smaller emittances one can obtain much higher $\gamma\gamma$ luminosity [12]. Fig.10 shows dependence of the $\gamma\gamma$ luminosity on the horizontal beam size. Solid curves correspond to the case where the vertical emittance is the same as in TESLA(500), ILC(500) projects (see Table 1). Dashed curves represent the case where the vertical beam sizes are as small as possible and are determined only by the minimum distance between the interaction and conversion points ($\sigma_y \sim b/\gamma$), where $b_{min} \sim 3\sigma_z + 0.08E[\text{TeV}] \text{ cm}$. The second term is the half length of the conversion region determined by nonlinear effects in Compton scattering.

One can see that all curves follow their natural behavior: $L \propto 1/\sigma_x$, with the exception of ILC at $2E_0 = 1$ GeV where the effect of coherent pair creation is seen. This means that at the same colliders the $\gamma\gamma$ luminosity can be increased almost by two orders. Even with one order improvement, the number of “interesting” events (the Higgs, charged pairs) at photon colliders will be larger than that in e^+e^- collisions by more than one order. This is a nice goal and motivation for photon colliders.

There are several ways of decreasing transverse beam emittances (their product): optimization of storage rings (with long wigglers) and low-emittance guns (with merging many beams with low emittances). Here progress is certainly possible. Moreover, there is one method which allows further decrease of beam cross sections by two orders in comparison with current designs. It is laser cooling [13-14]. In this method the electron beam at an energy of about 5 GeV is collided 1-2 times with a powerful laser flash, losing in each collision a large fraction ($\sim 90\%$) of its energy to radiation, with reacceler-

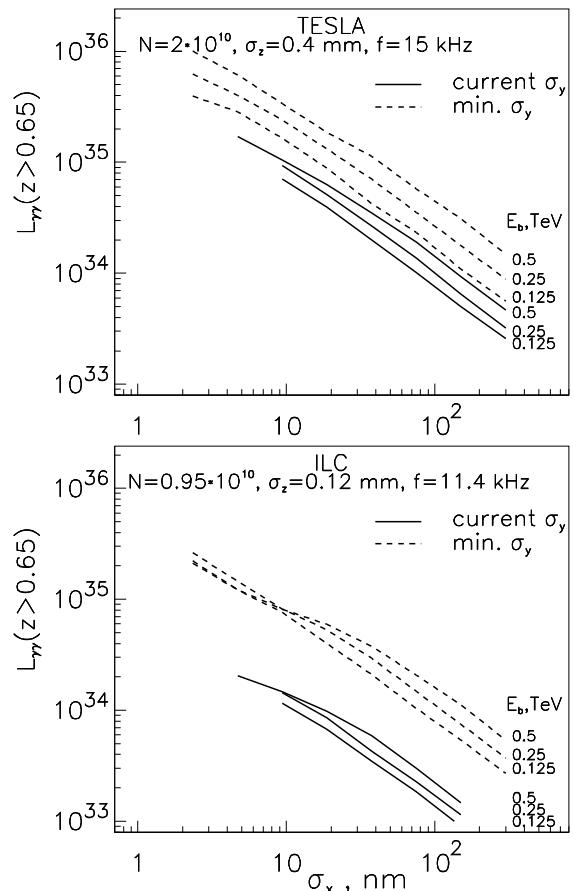


Figure 10: Dependence of $\gamma\gamma$ luminosity on the horizontal beam size for TESLA and ILC at various energies. Solid curves for nominal vertical beam size, dashed curves for minimum vertical beam size determined by the minimum distance between the conversion and interaction points.

ation between cooling sections. The physics of the cooling process is the same as in a wiggler. The required flash energy is about 10 Joules. This scheme can be realized, in principle, already. If this upgrading of luminosity is to be done in 15 years from now then, certainly, it will be no problem. For example, the peak power of lasers increased during the last ten years by 4 orders of magnitude. All laser technologies required for photon colliders are being developed actively now for other applications.

5 CONCLUSION

Prospects of photon colliders for particle physics are great; the physics community should not miss this unique possibility.

Acknowledgements

I would like to thank all my colleagues for joint work, useful discussions and support of this direction. Special thanks to A.Sessler for his strong promotion of gamma-gamma colliders [6],[15].

References

- [1] I.Ginzburg, G.Kotkin, V.Serbo, V.Telnov, *Pizma ZhETF*, **34** (1981) 514; *JETP Lett.* **34** (1982) 491.
- [2] I.Ginzburg, G.Kotkin, V.Serbo, V.Telnov, *Nucl. Instr. & Meth.* **205** (1983) 47.
- [3] I.Ginzburg, G.Kotkin, S.Panfil, V.Serbo, V.Telnov, *Nucl. Instr. & Meth.* **219** (1984) 5.
- [4] V.Telnov, *Nucl. Instr. & Meth.A* **294** (1990) 72.
- [5] V.Telnov, *Nucl. Instr. & Meth.A* **355** (1995) 3.
- [6] *Proc.of Workshop on $\gamma\gamma$ Colliders*, Berkeley CA, USA, 1994, *Nucl. Instr. & Meth. A* **355** (1995) 1-194.
- [7] *Zeroth-Order Design Report for the Next Linear Collider* LBNL-PUB-5424, SLAC Report 474, May 1996.
- [8] *Conceptual Design of a 500 GeV Electron Positron Linear Collider with Integrated X-Ray Laser Facility* DESY 79-048, ECFA-97-182. R.Brinkmann et al., *Nucl. Instr. & Meth. A* **406** (1998) 13.
- [9] *JLC Design Study*, KEK-REP-97-1, April 1997. I.Watanabe et. al., KEK Report 97-17.
- [10] V.Telnov, *Proc. of 2 nd Intern. Workshop on e-e- interactions at TeV energies*. Santa Cruz, California, USA, Sept, *Int.J.Mod.Phys. A* **13** (1998) 2399, e-print:hep-ex/9802003.
- [11] P.Chen, V.Telnov, *Phys. Rev. Lett.*, **63** (1989) 1796.
- [12] V.Telnov, *Proc. of ITP Workshop “Future High energy colliders”* Santa Barbara, USA, October 21-25, 1996, AIP Conf. Proc. No 397, p.259-273; e-print: physics/ 9706003.
- [13] V.Telnov, *Proc. of ITP Workshop “New modes of particle acceleration techniques and sources”* Santa Barbara, USA, August 1996, AIP Conf. Proc. No 396, p.121, *Phys.Rev.Lett.*, **78** (1997) 4757, erratum ibid 80 (1998) 2747, e-print: hep-ex/9610008.
- [14] V.Telnov, *Proc. 15 ECFA Workshop on Quantum aspects of beam physics*, Monterey, USA, 4-9 Jan. 1998, Budker INP 98-33,e-print: hep-ex/9805002.
- [15] A.Sessler, Gamma ray colliders and muon colliders, *Physics Today*, **51** (1998) 48.